Available online at www.sciencedirect.com
ScienceDirect
Journal of Magnetic Resonance 191 (2008) 47–55
JMR Journal of Magnetic Resonance
www.elsevier.com/locate/jmr

Proximal magnetometry in thin films using βNMR

M. Xu [a], M.D. Hossain [b], H. Saadaoui [b], T.J. Parolin [c], K.H. Chow [d], T.A. Keeler [b], R.F. Kiefl [b,a,e], G.D. Morris [a], Z. Salman [a,1], Q. Song [b], D. Wang [b], W.A. MacFarlane [c,*]

[a] *TRIUMF, 4004 Wesbrook Mall, Vancouver, Canada V6T 2A3*
[b] *Department of Physics and Astronomy, University of British Columbia, Vancouver, Canada V6T 1Z1*
[c] *Department of Chemistry, University of British Columbia, Vancouver, BC, Canada V6T 1Z1*
[d] *Department of Physics, University of Alberta, Edmonton, Canada T6G 2G7*
[e] *Canadian Institute for Advanced Research, Toronto, Canada M5G 1Z8*

Received 20 July 2007; revised 22 November 2007
Available online 8 December 2007

Abstract

Low energy ion implantation of hyperpolarized radioactive magnetic resonance probes allows the NMR study of thin film heterostructures by enabling depth-resolved measurements on a nanometer lengthscale. By stopping the probe ions in a layer adjacent to a layer of interest, it is possible to study magnetic fields proximally. Here we show that, in the simplest case of a uniformly magnetized layer, this yields an unperturbed *in situ* frequency reference. We also discuss demagnetization contributions to measured shifts for this case. With a simple illustrative calculation, we show how a nonuniformly magnetized layer causes a strongly depth-dependent line broadening in an adjacent layer. We then give some experimental examples of resonance line broadening in heterostructures.

Keywords: Thin films; Beta detected; NMR

1. Introduction

Depth-resolved beta-detected NMR (βNMR) and low energy muon spin rotation (LEμSR) have recently been shown capable of measuring local magnetic fields in thin film samples [1,2]. With this advent, it has become important to consider some general features of the measurements. In both βNMR and LEμSR, the probe nuclei are implanted as a beam of charged particles into the sample at low energy (for βNMR, the typical range is 0.1–30 keV), and the detection is enabled by the anisotropic property of the weak interaction that causes the beta decay. The implantation energy, and hence the probe stopping range, can be modified by electrostatic deceleration. This opens the possibility for new types of measurements, e.g., on a thin film deposited onto a crystal substrate. Provided the film is not too thick, it is possible to range the probe ions into *and through* the film. The signal from ions stopping in the substrate may thus provide a convenient *in situ* reference signal for the measurement of shifts. Alternatively, one can cap the film of interest with a thin overlayer of a simple, unreactive material such as Ag or Au, and range the probe ions into the capping layer as a reference. The purpose of this paper is to show, on general grounds, how classical magnetostatic effects manifest themselves in such measurements. The results are critical to both the interpretation of experiments and in establishing the practical sensitivity limit of certain measurements. Specifically, with the recent demonstration of βNMR measurements in thin films [3–5], two different concerns arise: (1) what is the effect of demagnetization on the NMR signal from within a uniformly magnetized film, and (2) what is the effect of the magnetization of the film on the average

* Corresponding author.
E-mail address: wam@chem.ubc.ca (W.A. MacFarlane).
[1] Present address: Clarendon Laboratory, Department of Physics, Oxford University, Parks Road, Oxford OX1 3PU, UK.

1090-7807/$ - see front matter © 2007 Elsevier Inc. All rights reserved.
doi:10.1016/j.jmr.2007.11.022

internal field sensed in an adjacent layer, i.e., can demagnetization affect the measurement of the reference signal? We treat these questions in Sections 2 and 3, respectively.

We then turn to the case of nonuniform magnetization in a thin film, which can arise from many interesting phenomena such as magnetic domain formation, density wave magnetism, electronic phase separation, magnetic screening in a superconductor, or time-reversal symmetry breaking superconductivity that have been studied by various traditional forms of magnetic microscopy [6]. It can also originate from the morphology of a magnetized film, for example via grain boundaries or interface roughness [7]. In this context, it may be an advantage to implant the probe ions, not into the film of interest, but rather into the adjacent substrate or capping layer to study the film from a vantage point (very) nearby. For example, in the layer of interest, the spin–lattice relaxation time T_1 may be substantially shorter than the probe's radioactive lifetime, as is often the case in magnetic materials. This will be more common for ^{8}Li ($\tau = 1.2$ s) than for μ^+ with its much shorter lifetime (2.2 μs). Even if T_1 is long enough, magnetic inhomogeneity may yield an unobservably broad resonance. One may also want to avoid the possibility that the implanted probe may perturb the system of interest. For these reasons, it is interesting to consider what information might be obtained by "implanted ion proximal magnetometry" (IIPM). We note several experiments along these lines have already been accomplished using βNMR [4,8–10], and that IIPM is similar to NMR and EPR decoration experiments (the analogue of Bitter decoration of a superconductor) [11] and the use of adsorbed layers of hyperpolarized ^{129}Xe [12], but with the advantage of an easily controlled probe depth and a thin film geometry. We discuss this application in Section 4 and illustrate the results with experimental data in Section 5.

2. Inside a uniformly magnetized film

We begin by revisiting an old problem, that of demagnetizing fields, but here in the context of a thin film. The demagnetizing field is a contribution to the local field inside a magnetized material, due to the discontinuity of magnetization at the surface of the sample. It is thus dependent on the sample geometry. For a thin film where the total magnetic moment is extremely small, simply by virtue of the amount of material, it is perhaps surprising that this contribution to the field could be significant. Following the original treatment of the local electric field in a polarizable medium by Lorentz and Debye [13], the total local magnetic field is generally decomposed into four contributions,

$$H_{\rm tot} = H_0 + H_{\rm d} + H_{\rm L} + H_{\rm loc}, \tag{1}$$

H_0, the applied field, $H_{\rm d}$ the demagnetizing field, $H_{\rm L}$ the field due to the Lorentz cavity, and $H_{\rm loc}$ the magnetic field due to the immediate atomic neighbours of the site in question, i.e. those within the Lorentz cavity. In many cases, $H_{\rm loc}$ is often predominantly due to the local contact hyperfine interaction, but it may also contain significant contribution from nearby atomic magnetic dipoles. For simplicity, here we assume all four components in Eq. (1) are parallel. The Lorentz cavity (or sphere) is an imaginary boundary around the test point defined by the fact that magnetized material outside the cavity can be treated in the magnetic continuum approximation, while material inside the cavity must be treated atomically. It is thus $H_{\rm loc}$ that is of principal interest in the NMR of solids, and to extract it, one must be able to quantify $H_{\rm d}$ and $H_{\rm L}$. The demagnetizing field is just proportional to the bulk magnetization M,

$$H_{\rm d} = -NM, \tag{2}$$

where N is the dimensionless "demagnetization factor" which ranges from 0 to 1 in SI or 0 to 4π in the cgs sytsem, which we adopt hereafter. It has been calculated for ellipsoids, rectangular blocks and cylinders [14–16]. For nonellipsoidal samples, $H_{\rm d}$ is nonuniform, giving rise to a distribution of internal magnetic fields. For a spherical Lorentz cavity, one can calculate $H_{\rm L} = 4\pi M/3$, but there is no means to independently measure this quantity [17]. Note that for a spherical sample, $H_{\rm d} = -H_{\rm L}$, so that these terms simply cancel in $H_{\rm tot}$. Magnetic nuclei (of gyromagnetic ratio γ) will precess at the Larmor frequency

$$\omega = \gamma H_{\rm tot}.$$

The relative magnetic shift is

$$k = \frac{\omega - \gamma H_0}{\gamma H_0} \tag{3}$$

$$= \frac{H_{\rm d} + H_{\rm L} + H_{\rm loc}}{H_0}, \tag{4}$$

while the shift of interest is rather $k_{\rm c} = H_{\rm loc}/H_0$, so to obtain $k_{\rm c}$, one needs to account for $H_{\rm d}$ and $H_{\rm L}$. The effects of demagnetizing fields in the measurement of shifts and lineshapes in NMR have been considered numerous times [18–20], while their effects on the magnetic structure of thin magnetic films have also been considered, for example in Ref. [7]. In βNMR and LEμSR some new problems arise in correcting for demagnetization. The main purpose of this section is to obtain $k_{\rm c}$.

The implantation depth of both βNMR and LEμSR is variable between a few nanometers and a few hundred nm, while the typical beamspot for ^{8}Li$^+$ is about 3 mm diameter and somewhat larger for the low energy μ^+. A typical film dimension for βNMR is 8 mm by 10 mm by 100 nm thick, with the beam centred on this area. The aspect ratio ξ of the film (thickness to transverse dimension) is thus on the order of 10^{-5}. The demagnetization factor N for an infinite slab with perpendicular field is 4π. Corrections for a finite size slab can be obtained from the limit of an oblate ellipsoid [14],

$$N \approx 4\pi\left(1 - \frac{\pi}{2}\xi + 2\xi^2\right), \tag{5}$$

or alternatively from the expression for a flat cylinder [15]. The contribution to the relative shift k due to H_d is $-N\chi$, where χ is the dimensionless "volume" susceptibility, which for nonferromagnetic metals is 10^{-4} emu/cm^3 or less, so the leading order correction (to $N = 4\pi$) is 10^{-9} or less, which is negligible. It is thus reasonable to simply use $N = 4\pi$ to correct the shift k. This type of correction has been established in conventional NMR, in particular in proton NMR of single thin foils of transition metal hydrides [21]. In that work, the field direction was varied (from perpendicular to parallel) to isolate the demagnetization effect. We note that analogous measurements at high applied fields are not generally possible in βNMR and LEμSR, since H_0 must be parallel to the ion beam direction, to avoid deflection of the ion beam by the Lorentz force. However, at low H_0, transverse field experiments with the field in the plane of the film are possible [2]. The demagnetizing factor in this case is $N \approx \xi$, so the demagnetization contribution to the shift ($\Delta k \approx \chi\xi$) is negligible. At this point, we note that the thin cylinder result [15] clearly exhibits the type of inhomogeneity of the demagnetizing field that we can expect in the film, i.e. in the central region H_d is large, negative and relatively uniform, but it is significantly reduced in magnitude as the film's edge is approached. The corresponding distribution of magnetic fields would yield an asymmetrically broadened resonance, for example see Ref. [19]. However, this inhomogeneity is not important for thin films, where ξ is very small, as it is confined to within a few thicknesses of the outer edge. For example for $\xi = 10^{-5}$, H_d is within 1% of the bulk value except within about 20 thicknesses of the edge. Usually the beamspot is substantially smaller than the film area and centred on it, so we expect negligible broadening from this source. We note that corrections of k due to demagnetization are significant in the case of small H_{loc} and large χ. For both ^{8}Li and implanted muons, hyperfine couplings (thus H_{loc}) are generally rather small, so we can expect significant corrections to k for any material with large χ.

We continue with a sample calculation for the shift of ^{8}Li in two metals, nearly ferromagnetic palladium and nonmagnetic silver. In Pd χ is highly T dependent, with a value about 79×10^{-6} emu/cm^3 at 175 K. The correction to the measured shift due to H_d and H_L at this temperature is

$$\Delta k = 4\pi\left(1 - \frac{1}{3}\right)\chi = +661 \times 10^{-6} \tag{6}$$

which is a substantial fraction ($\sim 50\%$) of the observed value [4]. To extract the shift k_c due only to H_{loc} (in a metal called the Knight shift), we use $k_c = k + \Delta k$. Note that the sign of Δk is positive for a paramagnetic material, i.e. k_c will be more positive than the observed shift. For Pd the measured k is negative, so k_c is smaller in magnitude than k. For Ag, in contrast, $\chi \approx 9.3 \times 10^{-7}$ emu/cm^3 is much smaller and $\Delta k = +7.8 \times 10^{-6}$ which is less than 10% of the observed shift at room temperature [3]. This correction should be applied in order to obtain an accurate value for the Knight shift [3–5,22].

3. Adjacent to a uniformly magnetized film

We now consider the effect of a uniformly magnetized film on the field within an adjacent nonmagnetic (substrate or capping) layer. For a nonmagnetic material, $M \approx 0$, so the H_d, H_L and H_{loc} in Eq. (1) are all zero, and $H_{tot} = H_0$. However, when the nonmagnetic material is in close contact with a magnetized layer, the field of the adjacent layer will contribute, so

$$H_{tot} = H_0 + H_p + H_p^{loc}, \tag{7}$$

where H_p is the proximal field due to the magnetized layer, i.e. the purely classical dipolar field, and H_p^{loc} is a local contribution to H_{tot} that is the analogue of H_{loc}, but due to hybridization between electronic states of the magnetic and nonmagnetic layers at the interface. For example, H_p^{loc} is the term that yields the Knight shift of ^{129}Xe [12] and other species [23] adsorbed onto metals. In fact, H_p is just H_d calculated outside the material, but we reserve the notation H_d for the demagnetizing field within the magnetic material. Far from the film, H_p must have the form of a dipolar field due to the overall magnetic moment of the film, but the implanted probe ions stop within a few hundred nm of the film, making only the near-field relevant. Perhaps the simplest approach is to replace the uniformly magnetized layer by two sheets of fictitious magnetic charges in analogy with a parallel plate capacitor [24]. This yields a uniform demagnetization field within the magnetic film (between the plates) consistent with the above results. By analogy with the electric field *outside* a parallel plate capacitor [25], the magnetic field outside the film of aspect ratio ξ is

$$H_p = \xi M, \tag{8}$$

yielding an additional shift of the line which is again of the order $\xi\chi$, too small to measure. As an example, the magnetic field outside a Pd layer with $\xi = 10^{-5}$ at 40 kOe and room temperature (conditions relevant to Fig. 2) will be

$$H_p = 10^{-5} \times 63 \times 10^{-6} \times 40{,}000 \approx 25\ \mu\text{Oe}, \tag{9}$$

which is indeed negligible. Even adjacent to a layer of ferromagnetic iron, H_p would be less than 20 mOe. Fig. 2 demonstrates this for a 75 nm thick Pd film on $SrTiO_3$. The Larmor frequency in this experiment is established by measurements in a single crystal of MgO before and after the measurement in the film. The resonance in the $SrTiO_3$ substrate is split by the quadrupolar interaction into a set of satellite lines centred on ν_0. Taking the midpoint of the outer satellites as a measure of the field in the $SrTiO_3$ adjacent to the magnetized Pd, we find a shift relative to MgO of -0.2 ± 0.3 kHz, consistent with the calculation. So within the continuum approximation, the magnetic field changes abruptly at the interface of the thin film by an amount $H_d - H_p$ corresponding to the equivalent magnetic charge density at the surface. It is interesting to inquire microscopically over what length scale this change actually takes place. A simple calculation of the

field along the axis of a uniformly magnetized annular slab, is shown in Fig. 1. While the hole is not necessary for the calculation of H_d, it demonstrates that the demagnetizing field does not depend on literally being in the magnetic material. The figure illustrates that the transition at the surface occurs very sharply as $r_0 \to 0$ for this ideally flat surface, even though the z-axis is strictly *in vacuo*.

We conclude that, to a good approximation, the resonance frequency in an adjacent nonmagnetic layer will be *unaffected* by the magnetization of the film. The fact that H_p is much smaller than the analogous term H_d within the film is quite surprising. We note that H_p is simply the net dipolar field of the magnetized layer M. Other contributions to the proximal field in a heterostructure, distinct from H_p, are of substantial interest; for example, the magnetization of a ferromagnetic metal may penetrate into an adjacent nonmagnetic metal in an oscillatory manner, the analogue of the Ruderman–Kittel–Kasuya–Yosida (RKKY) effect in dilute magnetic alloys, giving rise to giant magnetoresistance in such heterostructures [9]. This type of proximal field is not included in H_p but rather in H_p^{loc}.

4. Adjacent to a nonuniformly magnetized film

An inhomogeneous magnetization $M(x, y)$ will yield an inhomogeneous proximal field H_p in the adjacent layer, giving rise to a broadening (and potentially a shift) of the resonance in that layer. We thus consider here how a nonuniformity in M is reflected in H_p. In Fig. 1, it can be seen that as the radius r_0 of the hole increases, H_p "leaks out" of the film over a z length scale about equal to r_0. In fact this phenomenon is generic and provides a well-known limit on spatial resolution in the magnetic microscopy of thin films [26]. Similar considerations apply to electrostatic force

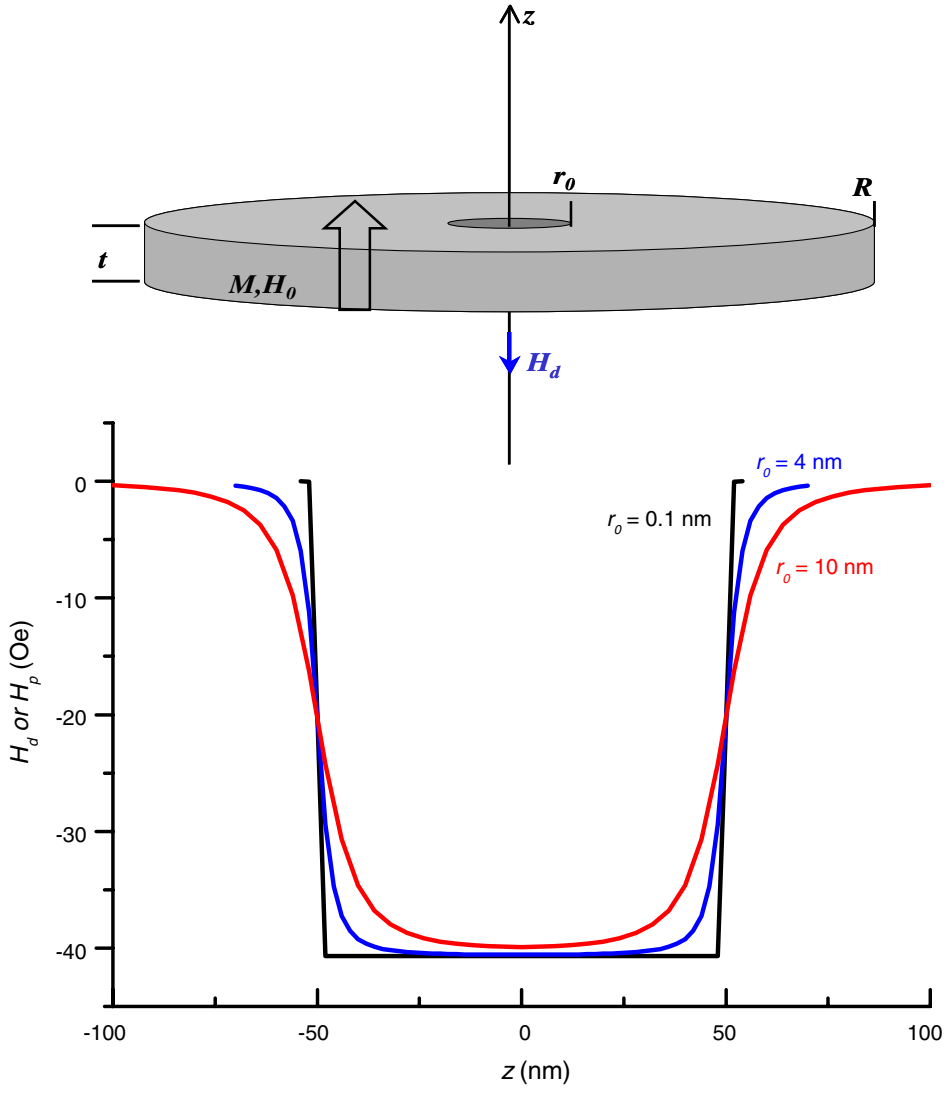

Fig. 1. The magnetic field profile through a thin cylindrical slab (on its axis) for a uniform magnetization perpendicular to the slab. The outer radius $R = 5$ mm , the film thickness $t = 100$ nm, and the origin is at the centre of the annulus. Profiles for three values of the radius of the central hole r_0 are shown. The magnetization is that of Pd at the conditions discussed in the text. As $r_0 \to 0$, the profile becomes sharply discontinuous at the film surfaces. Inside the film, the field equals $H_d = -4\pi M$, while outside the film, it is H_p.

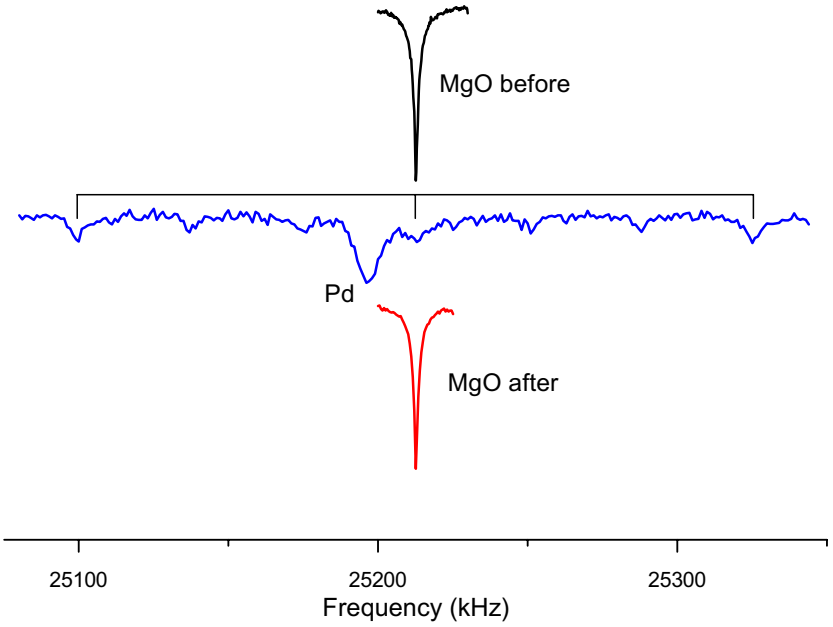

Fig. 2. The effect of a magnetized Pd film on the resonance in the substrate at room temperature and 40 kOe. Reference measurements of the resonance frequency ^{8}Li implanted into an MgO crystal before (top) and after (bottom) the measurement in the film. At the implantation energy of 28 keV, ^{8}Li stops in both the $SrTiO_3$ substrate and in the Pd. The quadrupole split spectrum in the $SrTiO_3$ is centred at the same frequency as the MgO, confirming that the magnetized Pd does not shift the signal from the adjacent substrate. The spectrum in the film also contains the negatively shifted signal from ^{8}Li that stop in the Pd layer.

microscopy [27]. Basically, the Fourier component of the magnetic field above a nonuniformly magnetized film at wavelength λ falls off as $\exp(-2\pi z/\lambda)$. Thus, to resolve a feature of lengthscale L in the magnetic layer, one needs to probe the magnetic near-field at a vertical distance $z \lesssim L$. This fact has also long been recognized in the field of magnetic recording technology [28]. In Fig. 1, the nonuniformity is the hole itself. Standard magnetostatics yield H_p as an integral of the dipolar fields of the magnetization or its equivalent volume and surface currents. The uniform component of H_p is represented by the surface term and was discussed in Section 3. For the case where the magnetization is normal to the plane of the film (parallel to H_0), the inverse problem inferring $M(x,y)$ from a measured $H_p(x,y)$ is discussed in detail in Refs. [26,29].

Implanted ion proximal magnetometry is analogous to techniques of near-field magnetic microscopy [6] such as the scanning squid, Hall probe arrays and magnetic force microscopy, but without any lateral spatial resolution, aside from the ability to steer the millimeter sized beamspot [30]. On the other hand, by stopping in an ultrathin overlayer, one can bring the probes much closer to the surface. Instead, the distribution of magnetic fields [31] $p(H_p)$ is sampled *randomly* over a large area. The implantation depth is easily variable from several hundred nm down to a few nm, e.g., see the recent demonstration of deceleration into a 4 nm thick gold overlayer [9]. The spatial resolution limit that is imposed by the probe distance z, thus spans the interesting nanometric length scale. Moreover, the sampling is spatially *local*, i.e. at the atomic scale, yielding a much higher intrinsic spatial resolution of the field distribution than with micron size scanning probes that report the net field integrated over a detector. Quantitative interpretation of an observed field distribution (resonance lineshape) will require modeling: postulating an intrinsic form for $M(x,y)$, possibly including interface roughness, calculating the distribution of $H_p(z)$, and averaging this over the implantation profile $p(z)$. Despite these complications, in the case that M is strongly temperature dependent, e.g., at a phase transition, one may easily correlate changes in the observed field distribution with $M(T)$.

Next we illustrate this process with a simple model calculation, i.e. for a thin uniform layer (thickness dz) having a magnetization corrugated as $M = M_0\cos(kx)$. This M is simple enough to have a closed form field distribution $p(H_p,z)$ and represents one component in a Fourier decomposition of an arbitrary M. It is also relevant to spontaneous sinusoidal inhomogeneities, for example the case of interfacial density waves [32]. By integrating the dipolar fields of the magnetization distribution, one obtains that, in a plane at height z above the layer, the magnetic field H_p is constant in magnitude and simply rotates in the x–z plane. The z component of H_p is thus distributed sinusoidally, i.e.

$$p(H_p,z) = \frac{1}{\pi\sqrt{H_{p0}(z)^2 - H_p^2}},$$

for $H_p \leqslant H_{p0}$ and zero elsewhere. The magnitude of the field at height z is $H_{p0}(z) = M_0\,\mathrm{d}z2\pi k\mathrm{e}^{-kz}$.

The implantation profile of an ion beam can be simulated in detail using Monte Carlo codes (e.g., inset of

Fig. 4), but it is often well approximated by a truncated gaussian,

$$\mathcal{P}(\tilde{z}) = A \exp\left[-\frac{1}{2}\left(\frac{\tilde{z}-R}{\delta R}\right)^2\right],$$

where $\tilde{z}$ is the depth, R is the most probable range, δR is the range straggling and A is a normalization factor. R and δR depend on the implantation energy, the overlayer material and the mass of the probe atoms. For low energy ion implantation δR is of the same order as R. $\mathcal{P}$ is zero for negative $\tilde{z}$, i.e. outside the sample. The net field distribution seen by the implanted probes stopping in an overlayer of thickness t is then

$$p(H_p) = \int_0^t d\tilde{z}\mathcal{P}(\tilde{z}) \times p(H_p, (t-\tilde{z})) \quad (10)$$

$$= \frac{A}{\pi}\int_0^t d\tilde{z}\frac{e^{-(\tilde{z}-R)^2/2\delta R^2}}{\sqrt{Ce^{-2k(t-\tilde{z})} - H^2}}, \quad (11)$$

where $C = (M_0\, dz\, 2\pi k)^2$. For $^8Li^+$ ions at 5.5 keV stopping in a silver overlayer, Monte Carlo simulations with TRIM.SP [33] predict $R \approx 20$ nm with $\delta R \approx 10$ nm. Assuming a 50 nm thick Ag layer on the magnetized sheet, the most likely stopping height is 30 nm. For this case, the field distribution $p(H_p)$ from Eq. (11) is shown (for several values of the corrugation wavelength λ) in Fig. 3, where we have assumed $M_0 = 50$ Oe. The calculated field distribution exhibits a remnant double peak structure from the singularities of the sinusoidal distribution, a feature characteristic of the simple corrugation that would not be expected generally, e.g., in the periodic structure of the vortex lattice of a superconductor (see below). While this calculation is too simple to yield a quantitative account of the resonance broadenings of the next section, it serves as a useful illustration of the generic behaviour, i.e. that the lengthscale of a magnetic inhomogeneity determines how far its effects propagate outside the material.

5. Examples

In this section, we present some experimental examples of line broadening in thin film heterostructures which are not fully understood at present, but where some insight can be gained in light of the results of the previous section. At the outset, we note that the detection scheme for both βNMR and LEμSR is based on the anisotropic property of weak decays, so that the spin polarization is detected via the high energy beta particles rather than by an induced voltage, as in conventional NMR. This nuclear detection scheme, makes the techniques very sensitive—in terms of signal per probe spin. In βNMR, resonances are measured as a loss of beta decay asymmetry, so they appear upside down compared to conventional NMR. More details can be found in Refs. [1,2].

First, we consider an inhomogeneous magnetization M due to the vortex state of a type-II superconducting layer with the probe ions stopping in a Ag overlayer. This type of measurement has been done at low magnetic field by LEμSR [34], but we present βNMR data here in high magnetic field. In the vortex state, the magnetic field in the superconductor becomes inhomogeneous due to the formation of flux vortices, which typically form a hexagonal lat-

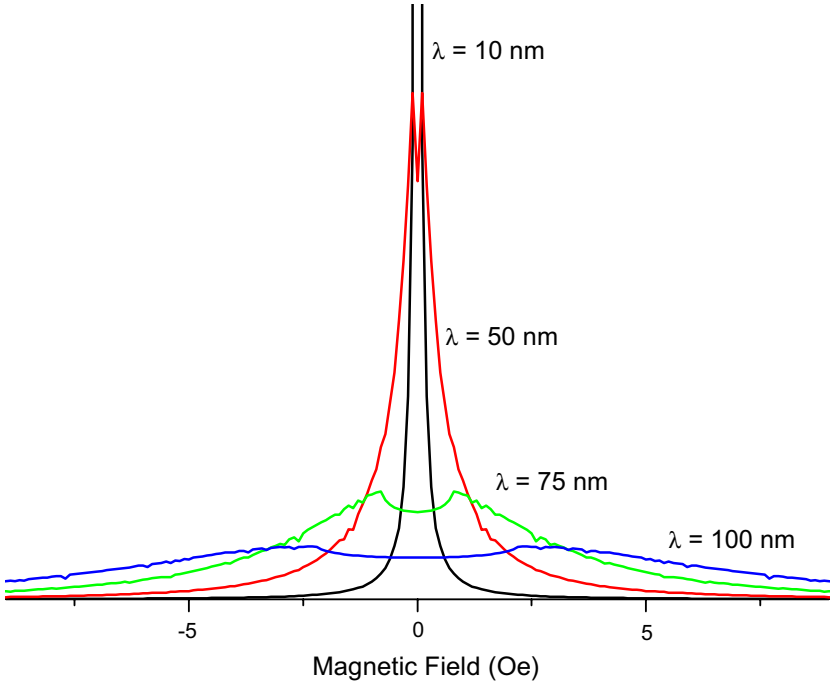

Fig. 3. Calculated field distribution for 5.5 keV $^8Li^+$ stopping in a 50 nm silver overlayer deposited on a thin layer with a corrugated magnetization: 50 Oe $\cos(kx)$ for various wavelengths of the corrugation $\lambda = 2\pi/k$. The two-peak structure originates in the sinusoidal distribution.

tice with vortex spacing $a = 489\ \text{Å}/\sqrt{B_0(T)}$. The length scale of the inhomogeneity is thus tunable via the applied field. Fig. 4 shows βNMR resonances for ^{8}Li implanted at 8 keV in a Ag overlayer (120 nm) capping a 300 nm thick film of *c*-axis oriented $YBa_2Cu_3O_7$ (YBCO7), a high temperature cuprate superconductor with superconducting critical temperature, $T_c \approx 90$ K. At this energy, the mean implantation depth in Ag is ~ 50 nm, and we expect all the ^{8}Li to stop in the Ag layer. The average vertical distance above the superconductor is then $\bar{z} = 70$ nm (see inset of Fig. 4). The resonance above T_c is narrow and shows similar temperature dependence to other Ag samples [3]. However, there is a dramatic broadening with a sharp onset at T_c, which is clearly due to the magnetic inhomogeneity in the vortex state. Measurements in bulk YBCO7 [35] show that the amplitude of the modulation in the magnetization $\Delta M \approx 50$ Oe in the superconducting layer at the applied field $H_0 = 13$ kOe, where the vortex spacing $a \approx 43$ nm. Here a represents the wavelength λ of the inhomogeneity of M, and ΔM is just a measure of the width of the distribution of $M(x, y)$. Scaling the inhomogeneity, we estimate the inhomogeneity in the field seen by the probe ions (the width of the distribution $p(H_p(\bar{z}))$) is $\Delta H_p \approx \Delta M \times \exp(-2\pi\bar{z}/a) = 2$ mOe, i.e., negligible and much smaller than the observed broadening which is $\Delta H_p \approx 10$ Oe. We conclude that there must be significant magnetic inhomogeneity in the superconducting films on length scales longer than a, i.e., long-wavelength disorder in the flux lattice. Similar conclusions were reached in EPR decoration experiments [36]. In fact long-range ordering of the vortex lattice is known to be unstable to the presence of any microscopic crystalline disorder [37], but it is likely that grain boundaries in the polycrystalline film are the main source of this long-wavelength disorder. For example, twin boundaries are known to modulate the vortex density in YBCO7 [38]. The grain size in the film is roughly 500 nm, so an inhomogeneity in M of 25 Oe on this lengthscale would be sufficient to explain the observed broadening. Experiments to test this conclusion are underway in capped single crystals which should have a much more ordered vortex state.

As a second example, Fig. 5 shows the broadening of the ^{8}Li resonance in two films of Au, one on a nonmagnetic $SrTiO_3$ substrate and the other on a 100 nm thick layer of Pd [4]. To interpret the broadening in the Au/Pd layer, we consider its structure. Atomic force microscopy indicates a RMS surface roughness of 1 nm for the Au layer, while spectroscopic ellipsometry measurements were consistent with a 2 nm roughness of the Au/Pd interface. At 300 K and 41 kOe, M of the Pd is about 2.6 Oe, while for Au it is an order of magnitude smaller. Even if we consider the Au/Pd interface as a thin layer with a modulated magnetization of amplitude about 2.6 Oe, the resulting field distribution will be too narrow to explain the broadening. We are thus led to consider that the magnetization is altered by the presence of the Au. In fact, a large enhancement of the magnetization has been observed in Au/Pd sandwich structures [39]. In addition to an enhanced magnetization, there

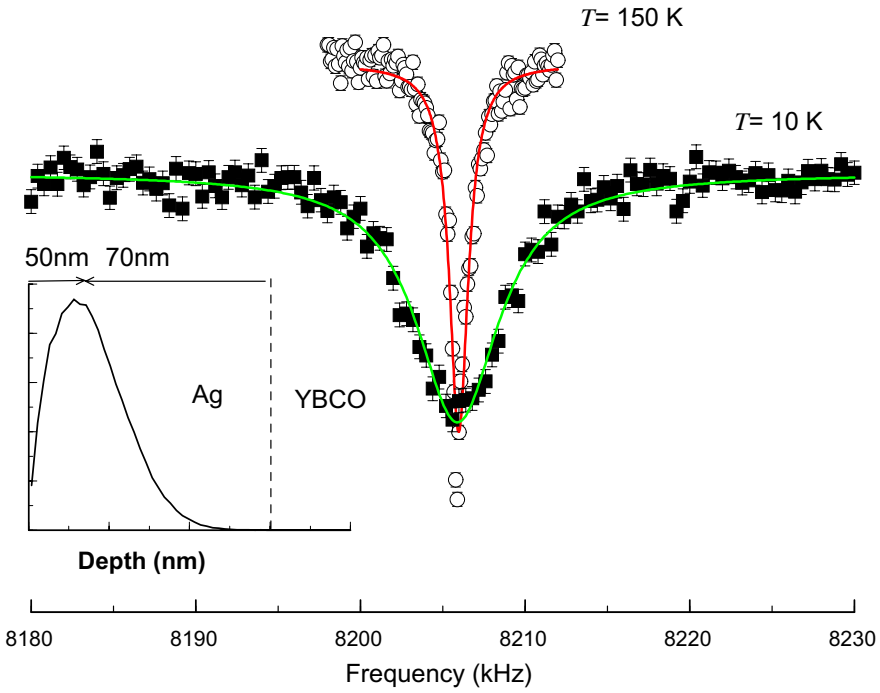

Fig. 4. A comparison of βNMR line broadening for ^{8}Li stopping in an Ag capping layer on a film of $YBa_2Cu_3O_7$. The top spectrum at 150 K is above T_c while the lower broadened line is deep in the vortex state. The excess broadening begins sharply at the superconducting transition and reflects the inhomogeneous magnetization in the vortex state at $H_0 = 13$ kOe. Inset: the implantation profile calculated using TRIM.SP.

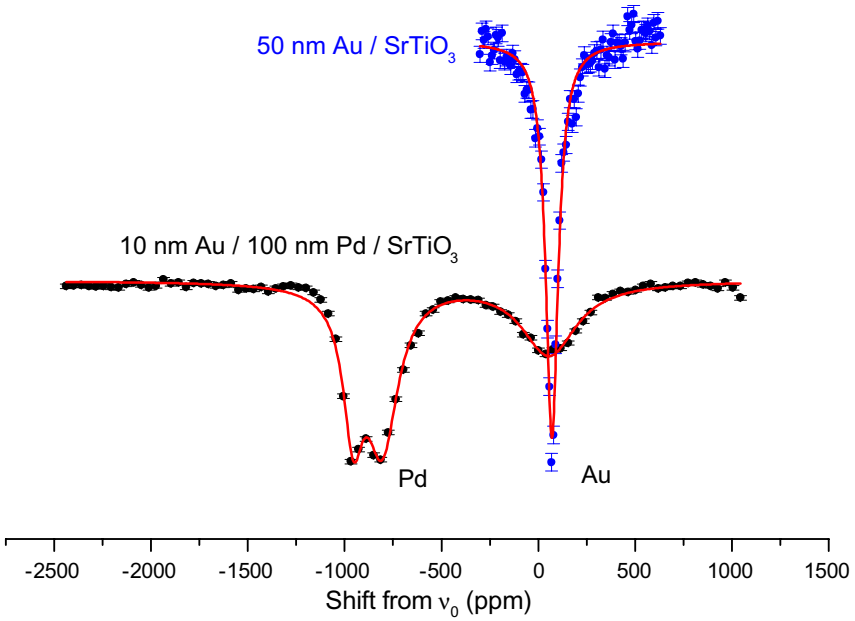

Fig. 5. A comparison of βNMR line broadening in two thin film heterostructures. The top data is for a 50 nm Au film on an $SrTiO_3$ substrate, and the bottom one is for a 100 nm Pd film on an $SrTiO_3$ substrate capped with a nominally 10 nm thick film of Au. The implantation energies were 10 and 13 keV, the temperatures 290 and 270 K, and the magnetic fields 30 and 41 kOe, respectively.

may be an additional contribution to the broadening from H_p^{loc}, due to RKKY polarization of the Au conduction band, as seen in Fe/Ag multilayer structures [9].

In this context, it is thus interesting to consider the magnetic field resolution of the technique. The observed resonance lineshape will be a convolution of the lineshape in the host material with the distribution of H_p. Au and Ag have been considered as overlayer materials, partly for their chemical inertness, but also for their high density which allows implantation into very thin layers. In these materials, the implanted ^{8}Li resonance is also extremely narrow, with linewidths of a fraction of an Oe, due to dipolar broadening by the small host lattice nuclear moments [3]. It is thus possible to detect shifts and broadenings of the resonance on the milliOe scale. Because βNMR and LEμSR use polarized implanted probes, enabling experiments at low H_0 [40], the above resolution is equally obtainable down to very low magnetic fields.

6. Summary

To summarize, we have considered aspects of the local magnetic field in thin film heterostructures that will generally be relevant to NMR experiments using low energy implanted ion probes, i.e. βNMR and LEμSR. We found that surface contributions within a uniformly magnetized thin film can make a significant contribution to observed magnetic shifts. However, the analogous field just outside such a film is negligible, so that ions stopped in an adjacent nonmagnetic layer may be used as a good *in situ* frequency reference. For the case of nonuniform magnetization, we calculated the field distribution outside a layer with a simple magnetic corrugation to illustrate the strongly depth dependent broadening caused by the exponential decay of the field. This fact will be important in the interpretation of depth-resolved NMR in thin film heterostructures and in the use of implanted ion proximal magnetometry to study magnetism in thin films.

Acknowledgments

We acknowledge R. Abasalti, B. Hitti, D.J. Arseneau and S. Daviel for technical assistance; D.E. MacLauglin for discussions and a careful reading of the manuscript; and W. Eckstein for the TRIM.SP code. This work was funded by NSERC Canada. We thank P. Fournier and H.-U. Habermeier for the samples.

References

[1] R.F. Kiefl, W.A. MacFarlane, P. Amaudruz, D. Arseneau, R. Baartman, T.R. Beals, J. Behr, J. Brewer, S. Daviel, A. Hatakeyama, B. Hitti, S.R. Kreitzman, C.D.P. Levy, R. Miller, M. Olivo, R. Poutissou, G.D. Morris, S.R. Dunsiger, R. Heffner, K.H. Chow, Y. Hirayama, H. Izumi, C. Bommas, E. Dumont, L.H. Greene, Nucl. Inst. Methods B 204 (2003) 682–688.
[2] P. Bakulé, E. Morenzoni, Contemp. Phys. 45 (2004) 203–225.
[3] G.D. Morris, W.A. MacFarlane, K.H. Chow, Z. Salman, D.J. Arseneau, S. Daviel, A. Hatakeyama, S.R. Kreitzman, C.D.P. Levy, R. Poutissou, R.H. Heffner, J.E. Elenewski, L.H. Greene, R.F. Kiefl, Phys. Rev. Lett. 93 (2004) 157601.
[4] T.J. Parolin, Z. Salman, J. Chakhalian, Q. Song, K.H. Chow, M.D. Hossain, T.A. Keeler, R.F. Kiefl, S.R. Kreitzman, C.D.P. Levy, R.I. Miller, G.D. Morris, M.R. Pearson, H. Saadaoui, D. Wang, W.A. MacFarlane, Phys. Rev. Lett. 98 (2007) 047601.
[5] Z. Salman, A.I. Mansour, K.H. Chow, M. Beaudoin, I. Fan, J. Jung, T.A. Keeler, R.F. Kiefl, C.D.P. Levy, R.C. Ma, G.D. Morris, T.J. Parolin, D. Wang, W.A. MacFarlane, Phys. Rev. B 75 (2007) 073405.

[6] E.g., S.J. Bending, Adv. Phys. 48 (1999) 449–535;
J.R. Kirtley, J.P. Wikswo Jr., Ann. Rev. Mat. Sci. 29 (1999) 117–148;
M.R. Koblischka, U. Hartmann, Ultramicroscopy 97 (2003) 103–112;
M.R. Freeman, B.C. Choi, Science 294 (2001) 1484–1488;
M. Tokunaga, Y. Tokunaga, T. Tamegai, Phys. Rev. Lett. 93 (2004) 037203.
[7] Y.-P. Zhao, G. Palasantzas, G.-C. Wang, J.Th.M. De Hosson, Phys. Rev. B 60 (1999) 1216–1226.
[8] Z. Salman, K.H. Chow, R.I. Miller, A. Morello, T.J. Parolin, M.D. Hossain, T.A. Keeler, C.D.P. Levy, W.A. MacFarlane, G.D. Morris, H. Saadaoui, D. Wang, R. Sessoli, G.G. Condorelli, R.F. Kiefl, Nano Lett. 7 (2007) 1551–1555.
[9] H. Luetkens, J. Korecki, E. Morenzoni, T. Prokscha, M. Birke, H. Glckler, R. Khasanov, H.-H. Klauss, T. lezak, A. Suter, E.M. Forgan, Ch. Niedermayer, F.J. Litterst, Phys. Rev. Lett. 91 (2003) 017204;
T.A. Keeler, Z. Salman, K.H. Chow, B. Heinrich, M.D. Hossain, B. Kardasz, R.F. Kiefl, S.R. Kreitzman, W.A. MacFarlane, O. Mosendz, T.J. Parolin, D. Wang, Phys. B 374–375 (2006) 79–82;
Z. Salman et al., Phys. Rev. B, (submitted for publication).
[10] R.I. Miller, D. Arseneau, K.H. Chow, S. Daviel, A. Engelbertz, M.D. Hossain, T. Keeler, R.F. Kiefl, S. Kreitzman, C.D.P. Levy, P. Morales, G.D. Morris, W.A. MacFarlane, T.J. Parolin, R. Poutissou, H. Saadaoui, Z. Salman, D. Wang, J.Y.T. Wei, Phys. B 374–375 (2006) 30–33.
[11] E.g., N. Bontemps, D. Davidov, P. Monod, R. Even, Phys. Rev. B 43 (1991) 11512–11514;
M. Wahlen, M. Rubsam, O. Dobbert, K.P. Dinse, Phys. C 185 (1991) 1797–1798;
R.I. Khasanov, Y.I. Talanov, G.B. Teitel'baum, Appl. Mag. Res. 14 (1998) 473–487;
A. Steegmans, R. Provoost, V.V. Moschalkov, H. Frank, G. Guntherodt, R.E. Silverans, Phys. C 259 (1996) 245–252;
Y. Maniwa, T. Mituhashi, K. Mizoguchi, K. Kume, Phys. C 175 (1991) 401–406.
[12] E.g., Y.Q. Song, B.M. Goodson, A. Pines, Spectroscopy 14 (1999) 26–33;
P. Gerhard, M. Koch, H.-J. Jansch, Compt. Ren. Phys. 5 (2004) 297–304;
D.N. Sears, L. Vukovic, C.J. Jameson, J. Chem. Phys. 125 (2006) 114708.
[13] H.A. Lorentz, The Theory of Electrons, Tuebner, Leipzig, 1909 (Chapter IV);
P. Debye, Phys. Z. 13 (1912) 97–100.
[14] J.A. Osborn, Phys. Rev. 67 (1945) 351–357;
E.C. Stoner, Phil. Mag. 36 (1945) 308–321.
[15] J.R. Eshbach, J. Appl. Phys. 34 (1963) 1298–1304.
[16] R.I. Joseph, E. Schlömann, J. Appl. Phys. 36 (1965) 1579–1593;
P.G. Akishin, I.A. Gaganov, J. Magn. Magn. Mater. 110 (1992) 175–180;
P. Rhodes, G. Rowlands, Proc. Leeds Philos. Soc. (1954) 191–210;
R.M. Bozorth, Ferromagnetism, Van Nostrand, New York, 1951.
[17] E.g., W.F. Brown Jr., Magnetostatic Principles in Ferromagnetism, North Holland, Amsterdam, 1962.
[18] W.C. Dickinson, Phys. Rev. 81 (1951) 717–731;
L.E. Drain, Proc. Phys. Soc. 80 (1962) 1380;
D.S. Schreiber, L.D. Graham, J. Chem. Phys. 43 (1965) 2573–2574;
G.C. Carter, L.H. Bennett, D.J. Kahan, Metallic shifts in NMR, in: B. Chalmers, J.W. Christian, T.B. Massalski (Eds.), Progress in Materials Science, vol. 20, Pergamon, Oxford, 1977 (vol. I, Chapter 5).
[19] G. Mozurkewich, H.I. Ringermacher, D.I. Bolef, Phys. Rev. B 20 (1979) 33–38.
[20] I. Bakonyi, P. Panissod, K. Tompa, Phys. Stat. Sol. 111 (1982) 59–64.
[21] S. Kazama, Y. Fukai, J. Less Common Met. 53 (1977) 25–33;
S. Kazama, Y. Fukai, J. Phys. Soc. Jpn. 42 (1977) 119–127.
[22] M. Mihara, S. Kumashiro, K. Matsuta, Y. Nakashima, H. Fujiwara, Y.N. Zheng, M. Ogura, H. Akai, M. Fukuda, T. Minamisono, Hyp. Int. 158 (2004) 361–364.
[23] P.-K. Wang, J.-P. Ansermet, S.L. Rudaz, Z. Wang, S. Shore, C.P. Slichter, J.H. Sinfelt, Science 234 (1986) 35–41.
[24] E.g., J.F. Cochran, B. Heinrich, Applications of Maxwell's Equations, Simon Fraser University, 2004, <http://www.sfu.ca/physics/associate/emeriti/cochran/MAXoutline.html/>.
[25] G.W. Parker, Am. J. Phys. 70 (2002) 502–507.
[26] B.J. Roth, N.G. Sepulveda, J.P. Wikswo Jr., J. Appl. Phys. 65 (1989) 361–372.
[27] S. Gómez-Mõnivas, J.J. Sáenz, R. Carminati, J.J. Greffet, Appl. Phys. Lett. 76 (2000) 2955–2957;
S. Lányi, M. Hruskovic, J. Phys. D 36 (2003) 598–602.
[28] D. Guarisco, Z. Li, W.E. Higgins, K. Saito, Y. Wu, A. LeFebvre, J. Appl. Phys. 99 (2006) 08Q908;
R.L. Wallace Jr., Bell Syst. Tech. J. 30 (1951) 1145–1173.
[29] S. Tan, Y.P. Ma, I.M. Thomas, J.P. Wikswo Jr., IEEE Trans. Magn. 32 (1996) 230–234.
[30] Some lateral resolution may be achieved using a patterned overlayer that is correlated with the magnetization structure.
[31] The distribution p of the magnetic field $H_p(x,y;z)$ in the measurement plane at z is

$$p(H,z) = \frac{1}{A}\int_A \delta(H - H_p(x,y;z))\mathrm{d}x\,\mathrm{d}y, \tag{12}$$

where δ is the Dirac delta function, and A is the area of integration. If H_p is periodic, as in the vortex lattice, then one can restrict the integration to the 2D unit cell.
[32] E.g., R.V. Coleman, B. Drake, P.K. Hansma, G. Slough, Phys. Rev. Lett. 55 (1985) 394–397;
P.T. Sprunger, L. Petersen, E.W. Plummer, E. Laegsgaard, F. Besenbacher, Science 275 (1997) 1764–1767.
[33] W. Eckstein, Computer Simulation of Ion–Solid Interactions, Springer, Berlin, 1991.
[34] Ch. Niedermayer, E.M. Forgan, H. Glückler, A. Hofer, E. Morenzoni, M. Pleines, T. Prokscha, T.M. Riseman, M. Birke, T.J. Jackson, J. Litterst, M.W. Long, H. Luetkens, A. Schatz, G. Schatz, Phys. Rev. Lett. 83 (1999) 3932–3935.
[35] J.E. Sonier, J.H. Brewer, R.F. Kiefl, Rev. Mod. Phys. 72 (2000) 769–811.
[36] M. Pozek, H.-U. Habermeier, A. Maier, M. Mehring, Phys. C 269 (1996) 61–70.
[37] A.I. Larkin, Zh. Eksp. Teor. Fiz. 58 (1970) 1466–1470, [Sov. Phys. JETP 31 (1970) 784–786].
[38] G.J. Dolan, G.V. Chandrashekhar, T.R. Dinger, C. Feild, F. Holtzberg, Phys. Rev. Lett. 62 (1989) 827–830.
[39] M.B. Brodsky, A.J. Freeman, Phys. Rev. Lett. 45 (1980) 133–137.
[40] Z. Salman, E.P. Reynard, W.A. MacFarlane, K.H. Chow, J. Chakhalian, S. Kreitzman, S. Daviel, C.D.P. Levy, R. Poutissou, R.F. Kiefl, Phys. Rev. B 70 (2004) 104404;
Z. Salman, R.F. Kiefl, K.H. Chow, M.D. Hossain, T.A. Keeler, S.R. Kreitzman, C.D.P. Levy, R.I. Miller, T.J. Parolin, M.R. Pearson, H. Saadaoui, J.D. Schultz, M. Smadella, D. Wang, W.A. MacFarlane, Phys. Rev. Lett. 96 (2006) 147601.